Journal of Alloys and Compounds, *177* (1991) 311–320
JAL 0077

High coercivity sintered Pr–Fe–B–Cu magnets using the hydrogen decrepitation process

R. N. Faria, J. S. Abell and I. R. Harris
School of Metallurgy and Materials, University of Birmingham, Edgbaston, B15 2TT (U.K.)

(Received June 25, 1991)

Abstract

Sintered permanent magnets based on the compositions $Pr_{20.5}Fe_{73.8}B_{3.7}Cu_2$ and $Pr_{16.9}Fe_{79.1}B_4$ have been prepared using the hydrogen decrepitation process. For particular processing conditions, annealing the magnets at 1000 °C resulted in an increase in ${}_iH_c$ from 11 to around 20 kOe for both alloys. Sintered and furnace-cooled magnets exhibited higher intrinsic coercivities than the quenched magnets. The possibility of changing the easy direction of magnetization from the tetragonal *c*-axis to easy basal plane during hydrogen absorption has also been investigated as a means of producing radially anisotropic permanent magnets using the isostatic pressing method.

1. Introduction

Hydrogen decrepitation (HD) has been applied in the processing and characterization of Nd–Fe–B sintered permanent magnets in this laboratory over the past seven years [1–5]. Recently, great interest has arisen in Pr–Fe–B magnets due to the absence of a spin reorientation at lower temperatures when compared with Nd–Fe–B magnets [6] and hence better magnetic characteristics at low temperatures. The addition of elements such as copper, silver, gold or palladium has led to alloys with good magnetic properties in the form of hot-pressed and hot-rolled magnets [7–9]. Very recently, the $Pr_{20.5}Fe_{73.8}B_{3.7}Cu_2$ alloy has been found to exhibit ${}_iH_c$ values of 10–12 kOe in the cast ingots after annealing [10]. It has also been reported [11, 12] that $Pr_2Fe_{14}B$ when in the hydride form changes its easy direction of magnetization from the tetragonal *c*-axis to easy basal plane which, in practice, could produce radially anisotropic magnets. In the present work, sintered magnets of compositions $Pr_{20.5}Fe_{73.5}B_{3.7}Cu_2$ and $Pr_{16.9}Fe_{79.1}B_4$ have been prepared via the HD process and in view of the changes observed in the hot-pressed ingots [7] the effect of annealing on their coercivity has been studied. The possibility of producing radially aligned magnets was also investigated.

2. Experimental details

The chemical analyses of the alloys designated I and II, are given in Table 1. The copper-containing composition was chosen because it exhibited

0925-8388/91/$3.50

TABLE 1

Chemical analyses of the as-cast alloys

Alloy description	wt.%				at.%
	Pr	Fe	B	Cu	
(I) Pr-rich	40.0	Balance	0.60	1.60	$Pr_{20.5}Fe_{73.8}B_{3.7}Cu_2$
(II) Cu-free [7]	34.8	Balance	0.63	–	$Pr_{16.9}Fe_{79.1}B_4$

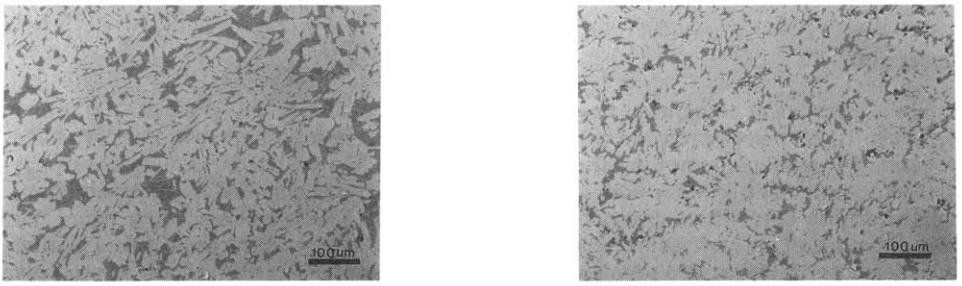

(a) (b)

Fig. 1. Optical metallograph showing a general view of the microstructure of an as-cast ingot of the alloys: (a) I and (b) II.

good magnetic properties in the cast and hot-pressed states and the copper-free alloy was chosen for comparison. The as-cast microstructures of the starting alloys with the familiar columnar grain structure are shown in Figs. 1(a) and (b). Phase analysis reveals that the alloys are composed of the matrix phase $Pr_2Fe_{14}B$, praseodymium-rich phase in the grain boundaries, free-iron and the $Pr_{1+\epsilon}Fe_4B_4$ boride phase in II but not in I. A detailed study of phase composition is given in ref. 10.

In order to establish the optimum milling conditions, a study of the relationship between the magnetic properties of the sintered magnets and the milling time was carried out for alloys I and II. Small pieces of the bulk ingot were placed in a stainless steel hydrogenation vessel which was evacuated to backing-pump pressure and hydrogen was then introduced to a pressure of 10 bars. The hydrogen absorption process occurred after a short incubation period of around 3–5 min. The decrepitated material was then transferred to a "roller" ball-mill under a protective atmosphere and milled for several hours using cyclohexane as the milling medium. The resultant fine powder was then dried and encapsulated in a small cylindrical rubber bag, pulsed at a magnetic field of 2400 kA m^{-1} and isostatically pressed at 1400 kg cm^{-2}. The consequent green compacts were then vacuum sintered at 1060 °C for 1 h. Some of the samples were slow-cooled in the furnace and others were fast-cooled by removing the furnace (cooling rates of approximately 3.5 and 100 °C min^{-1} respectively). A detailed description of the powder

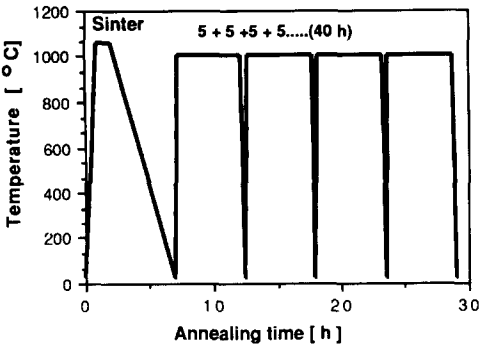

Fig. 2. Heat sequence for the magnets of alloys I and II.

and magnet production by the HD process has been given in refs. 2–4. Density measurements were carried out by a displacement method using a sensitive balance and diethylphthalate. The sintered magnets were then pulsed in a magnetic field of 2400 kA m^{-1} and their second quadrant demagnetization curves determined. For comparison with the as-sintered condition, the magnets were then annealed under vacuum at 1000 °C for 24 h (also furnace cooled) and their magnetic properties were re-measured.

A more detailed post-sintering annealing treatment was also carried out. This study consisted of fast heating to 1000 °C and then quenching at 5 h intervals (Fig. 2). In order to investigate the magnetic properties in the X and Y directions (radial directions), cylindrical magnets were cut into a cubic shape using a diamond saw.

3. Results and discussion

The effects of milling time are shown in Figs. 3–6. The most striking feature of these graphs is the variation of intrinsic coercivity with the milling time for the annealed samples. Alloy I exhibits a remarkable increase in ${}_iH_c$ in the powder milled for 9 h. In the same way, alloy II also exhibits a dramatic enhancement in ${}_iH_c$ after annealing but at a significantly longer milling time (27 h). For alloy I, ${}_iH_c$ stays high after the peak whereas for alloy II it falls to around the initial values. Another distinct feature of alloy I is that, even for as-crushed material with a coarse particle size (zero milling time in Fig. 3), the magnet exhibits appreciable coercivity and this can be attributed to the higher proportion of grain boundary phase in this material. The same investigation carried out for the corresponding neodymium alloys showed no peak in ${}_iH_c$ and a small increase in the general magnetic properties with annealing.

It has been suggested that, in the studies [8–10] on the cast alloys, annealing at 1000 °C increases ${}_iH_c$ by eliminating free iron and slow-cooling further increases the magnetic properties by enhancing the smoothness of the grain boundaries due to a low-temperature eutectic reaction. Contributions

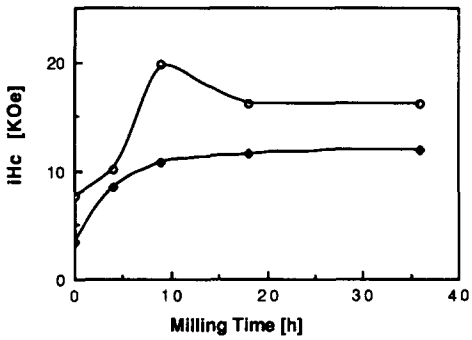

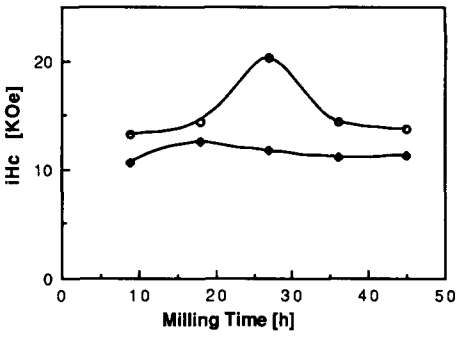

Fig. 3. Variation of ${}_iH_c$ with the milling time for slow-cooled magnets of alloy I. (◆: as-sintered, O: annealed 1000 °C, 24 h).

Fig. 4. Variation of ${}_iH_c$ with the milling time for slow-cooled magnets of alloy II. (◆: as-sintered, O: annealed 1000 °C, 24 h).

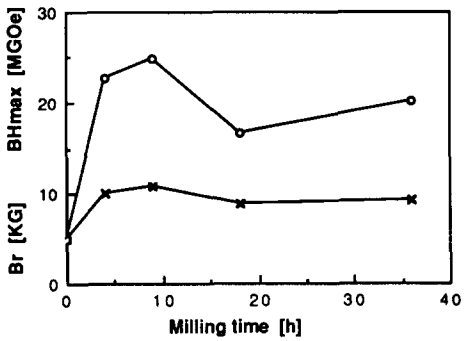

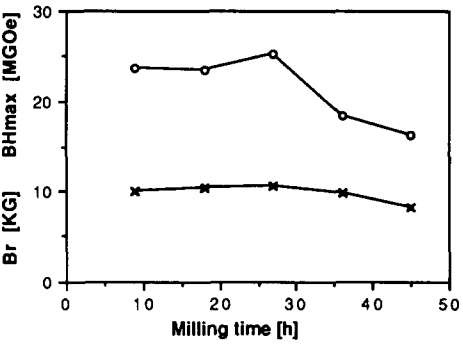

Fig. 5. Variation of B_r and BH_{max} with the milling time for slow-cooled and annealed (1000 °C for 24 h) samples of alloy I. (O: BH_{max}, x: B_r).

Fig. 6. Variation of B_r and BH_{max} with the milling time for slow-cooled and annealed (1000 °C for 24 h) samples of alloy II. (O: BH_{max}, x: B_r).

to the behaviour of ${}_iH_c$ in the sintered magnets include (1) the milled particle size and hence the subsequent grain size of the sintered magnet, (2) the coverage and thickness of the praseodymium-rich grain boundary material, (3) the smoothness of the grain boundaries and (4) the removal of any residual free iron. It is not clear at this juncture, however, why there is a peak in the behaviour of ${}_iH_c$ for both alloys. Microstructural studies are underway in an attempt to explain the coercivity behaviour observed in this work.

Figures 7 and 8 show how the intrinsic coercivity, remanence and energy product of magnets made from alloys I and II are affected by the annealing time in the sequence shown in Fig. 2. This heat treatment was chosen in order to diminish any influence of a low-temperature eutectic reaction and hence to study the effect of annealing at 1000 °C. For alloy I there is no

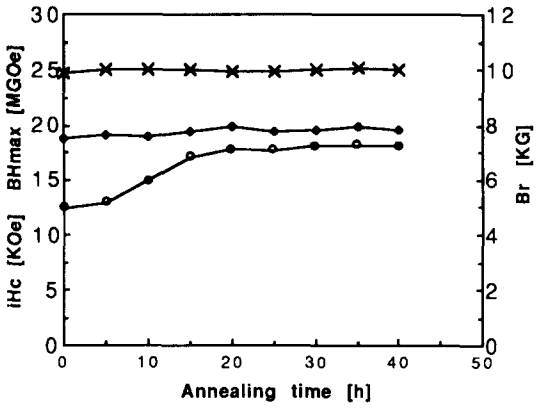

Fig. 7. Variation of B_r, $_iH_c$ and BH_{max} with annealing time for magnets of alloy I, using the heat sequence of Fig. 2. (◆: BH_{max}, x: B_r, ○: $_iH_c$).

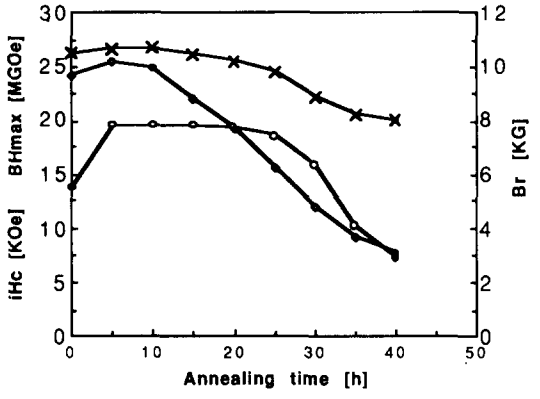

Fig. 8. Variation of B_r, $_iH_c$ and BH_{max} with annealing time for magnets of alloy II, using the heat sequence of Fig. 2. (◇: BH_{max}, x: B_r, ○: $_iH_c$).

significant change in B_r, $_iH_c$ or BH_{max} after 15 h and for alloy II these properties exhibit a significant deterioration at long annealing times.

The influence of the sintering temperature of the B_r values of magnets of alloy II is shown in Fig. 9. These values are rather lower than those obtained in the corresponding hot-pressed magnets (12.6 kG) [7]. Jiang *et al.* [13] have shown that Pr–Fe–B magnets prepared via HD and sintered in flowing argon have a tendency to retain some residual hydrogen, leading to a decrease in the density due to lattice expansion and to the appearance of pores, resulting in reduced remanence and consequently the energy product. Although in this work the magnets were vacuum sintered and showed higher densities as can be seen in Fig. 9 they still exhibit low remanence values compared with the hot-pressed material but this can be attributed to the "squeezing out" of the praseodymium-rich material during the hot-pressing operation. Demagnetization curves for the annealed magnets (24 h, 1000 °C) are shown in the Figs. 10–12. Alloy I is slightly inferior to alloy II (before

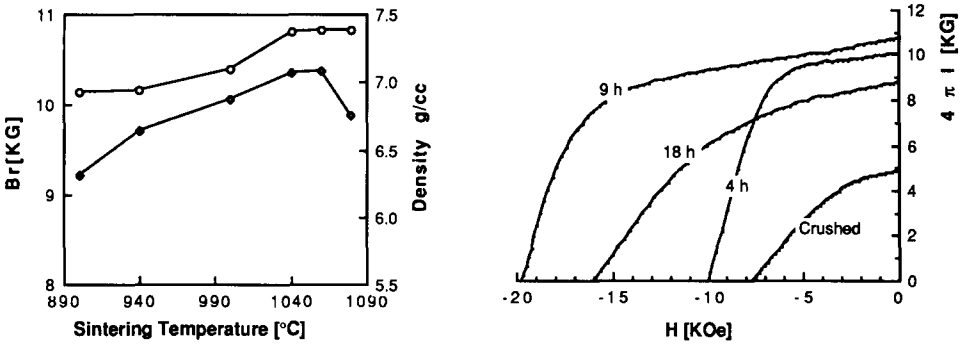

Fig. 9. Variation of remanence and density with the sintering temperature. Quenched samples of alloy II. (○: density, ◇: B_r).

Fig. 10. The demagnetization curves for annealed (1000 °C, 24 h) slow-cooled magnets of alloy I after various milling times.

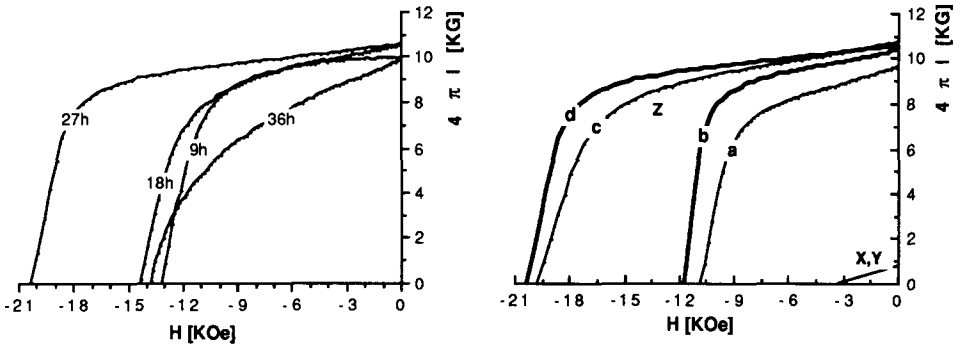

Fig. 11. The demagnetization curves for annealed (1000 °C, 24 h) slow-cooled magnets of alloy II after various milling times.

Fig. 12. The demagnetization curves for slow-cooled magnets of alloys I (a – sintered, c – annealed) and II (b – sintered, d – annealed). Curves a, b, c and d measured in *Z* direction (alignment) and *X*, *Y* radial direction for alloy I.

and after annealing) and this is consistent with the greater praseodymium content in the former.

It has been reported by Pourarian, Huang and Wallace [11], that $Pr_2Fe_{14}BH_5$ (HD pressure: 60 atm) exhibits planar anisotropy and Lin *et al.* [12] demonstrated that the tetragonal *c*-axis of the HD powder lies in the plane perpendicular to the magnetic field direction during alignment and the subsequent dehydrogenation and sintering does not change this radial alignment. Their powder was uniaxially pressed with the field direction perpendicular to the press direction using hydrogen-decrepitated and hammer-milled material. In the present work, an isostatic pressing method has been used which removes the influence of pressing on the magnetic properties of the magnet.

Figure 12 also shows the demagnetization curve in the *X*,*Y* (radial) directions for hydrogen-decrepitated (alloy I) magnets aligned and subse-

quently pressed in an isostatic press. Figure 13 shows a typical microstructure of a magnet made from alloy I. All the magnets prepared via the HD process showed uniaxial anisotropy in the direction of alignment Z. The absence of radial alignment can be attributed to the lower hydrogenation pressure of 10 bar used in the present work giving a lower hydrogen content than that reported in ref. 11 and lattice parameters measurements using X-ray diffraction revealed that the alloy decrepitated at 10 bar had a formula unit of $Pr_2Fe_{14}BH$ assuming a linear variation of volume with hydrogen content.

The X-ray diffraction pattern shown in Fig. 14 (similar to those of ref. 7) indicates clearly that the direction of magnetization of the HD sintered magnets lies in the c-axis which is consistent with the magnetic measurements. According to Zhou *et al.* [14] well aligned samples show only three strong peaks: (004), (105) and (006), where the (004) and (006) are perpendicular to the easy direction [001] in the tetragonal crystal structure of the $Nd_2Fe_{14}B$ phase, the (105) is tilted by about 15° from the (00n) plane and the (006) reflection is the strongest one.

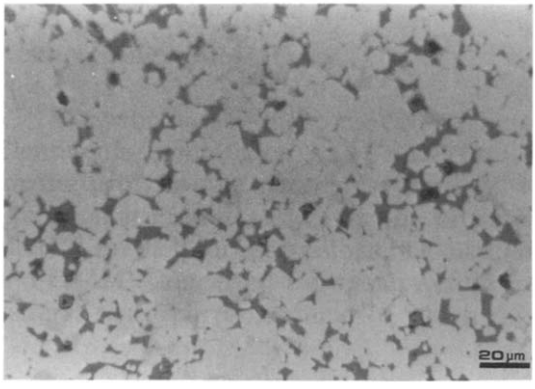

Fig. 13. Microstructure of a magnet of alloy I. Milling time 9 h.

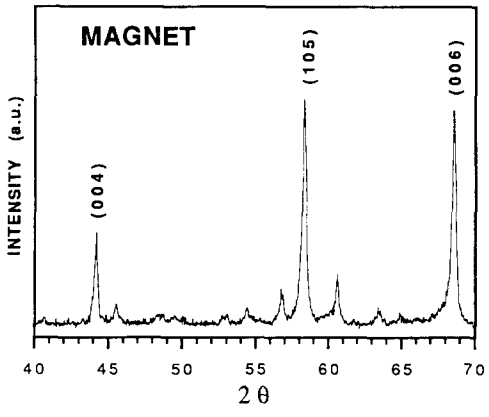

Fig. 14. X-ray diffraction pattern of a $Pr_{17}Fe_{79}B_4$ magnet prepared using the HD process.

TABLE 2

Comparison of various HD sintered permanent magnets

Alloy type	Ref.	Processing conditions	Heat treatment	B_r (kg)	$_iH_c$ (kOe)	BH (MG Oe)	d (g cm^{-3})	Alig
$Pr_{20.5}Fe_{73.8}B_{3.7}Cu_2$		HD = 10 bar, I.P.	1000 °C, 24 h, furn.	10.7	19.8	24.9	7.33	Uni
$Pr_{16.9}Fe_{79.1}B_4$		HD = 10 bar, I.P.	1000 °C, 24 h, furn.	10.6	20.3	25.3	7.10	Uni
$Pr_{17}Fe_{76.5}B_5Cu_{1.5}$	[7]	Hot pressing	1000 °C, 24 h, furn.	12.6	10.0	36.2	–	Uni
$Pr_{14}TbFe_{79}B_6$	[13]	HD = 60 atm, Ar flow	1100 °C, 1 h, quench	11.3	10.4	28.6	6.93	–
$Pr_{14}TbFe_{79}B_6$	[13]	Crushed + Mill, Ar F	1100 °C, 1 h, quench	12.3	16.6	33.5	7.34	–
$Pr_{17}Fe_{77.5}B_6Cu_{1.5}$	[12]	HD uniaxial press	–	7.5	8.5	10.5	–	Rad

HD: hydrogen decrepitated, IP: isostatically pressed, Uni: uniaxial, Rad: radial, furn: furnace cooled.

A summary of magnetic properties is given in Table 2. The higher remanence for the terbium-containing magnets can be ascribed to the higher anisotropy field which should result in better *c*-axis alignment.

4. Conclusions

(1) The intrinsic coercivity of Pr–Fe–B and Pr–Fe–B–Cu sintered magnets can be increased substantially by annealing.

(2) Magnets based on $Pr_{20.5}Fe_{73.8}B_{3.7}Cu_2$ when annealed exhibit a peak in ${}_iH_c$ at lower milling times than $Pr_{16.9}Fe_{79.1}B_4$ magnets.

(3) HD Pr–Fe–B–Cu magnets exhibit higher ${}_iH_c$ and lower B_r than hot-pressed magnets.

(4) Isostatically pressed magnets of Pr–Fe–B–Cu alloys produced by the HD process at 10 bar of H_2 are shown to exhibit uniaxial anisotropy.

Acknowledgments

Many thanks are due to the CNPq (Conselho Nacional de Desenvolvimento Científico e Tecnológico) and CNEN (Comissão Nacional de Energia Nuclear) for the provision of a research grant (R. N. Faria). Thanks are due to REP (Rare Earth Products Ltd.) for the provision of the alloys and to G. Mycock of REP for helpful discussions. Thanks are also due to the SERC, EURAM and CEAM (Concerted European Action on Magnets) for the support of the general research programme of which this work forms a part.

References

1 I. R. Harris, *J. Less-Common Met., 131* (1987) 245.
2 I. R. Harris, P. J. McGuiness, D. G. R. Jones and J. S. Abell, *Phys. Scr., T19* (1987) 435.
3 P. J. McGuiness and I. R. Harris, *J. Appl. Phys., 64* (10) (1988) 5308.
4 J. S. Abell and I. R. Harris, *IEEE Trans. Magn., MAG-24* (1988) 1620.
5 P. J. McGuiness, E. Devlin, I. R. Harris, E. Rozendaal and J. Ormerod, *J. Mater. Sci., 24* (1989) 2541.
6 S. Y. Jiang, J. X. Yan, B. M. Ma, S. G. Sankar and W. E. Wallace, *10th Int. Workshop on Rare-Earth Magnets and Their Applications, Kyoto, Japan, 16–19 May, 1989*, p. 457.
7 T. Shimoda, K. Akioka, O. Kobayashi and T. Yamagami, *IEEE Trans. Magn., MAG-25* (5) (1989) 4099.
8 W. C. Chang, C. R. Paik, H. Nakamura, N, Takahasi, S. Sugimoto, M. Okada and M. Homma, *IEEE Trans. Magn., MAG-26* (5) (1990) 2604.
9 T. Shimoda, K. Akioka, O. Kobayashi and T. Yamagami, *10th Int. Workshop on Rare-Earth Magnets and Their Applications, Kyoto, Japan, 16–19 May, 1989*, p. 389.

10 H. W. Kwon, P. Bowen and I. R. Harris, *5th Joint MMM–Intermag Conf., Pittsburgh, PA, June 18–21, 1991.*
11 F. Pourarian, M. Q. Huang and W. E. Wallace, *J. Less-Common Met., 120* (1986) 63.
12 C. H. Lin, C. J. Chen; C. D. Wu and W. C. Chang, *IEEE Trans. Magn., MAG-26* (5) (1990) 2607.
13 S. Y. Jiang, J. X. Yan, F. S. Li and C. L. Yang, *10th Int. Workshop on Rare-Earth Magnets and Their Applications, Kyoto, Japan, 16–19 May, 1989*, p. 409.
14 S. Z. Zhou, Y. X. Zhou and C. D. Graham Jr., *J. Appl. Phys., 63* (8) (1988) 3534.